ISSN 0029-3865

CBPF- CENTRO BRASILEIRO DE PESQUISAS FÍSICAS

Notas de Física

CBPF-NF-005/94

January 1994

Chaotic Dynamics of High Order Neural Networks*

Ney Lemke†, Jeferson J. Arenzon† and Francisco A. Tamarit[1]

[1]Centro Brasileiro de Pesquisas Físicas, Rua Dr. Xavier Sigaud, 150, 22290-180, Rio de Janeiro/RJ, Brasil

†Instituto de Física, Universidade Federal do Rio Grande do Sul, C.P. 15051, 91501-970, Porto Alegre/RS, Brasil

*E-mails: lemke@if1.ufrgs.br, arenzon@if1.ufrgs.br and tamarit@brlncc.bitnet

Abstract

The dynamics of an extremely diluted neural network with high order synapses acting as corrections to the Hopfield model is investigated. As in the fully connected case, the high order terms may strongly improve the storage capacity of the system. The dynamics displays a very rich behavior, and in particular a new chaotic phase emerges depending on the weight of the high order connections ϵ, the noise level T and the network load defined as the rate between the number of stored patterns and the mean connectivity per neuron $\alpha = P/C$.

PACS: 87.10+e – 75.10Hk

Key-words: Neural networks; Chaos; High order interactions.

1 INTRODUCTION

Neural networks have been subject of intense research in Statistical Mechanics in the last decade. However, besides the equilibrium properties that are reasonable well understood in the framework of spin glass theory, dynamical properties are hard to treat analytically and still requires further work. In the limit of low loading or focusing only in the first few time steps, several treatments [1] yielded important results, the challenge remaining for saturated networks [2]. Particularly, for extremely and asymmetrically diluted networks the dynamics can be exactly solved [3]. It is worth to stress here that both dilution and asymmetry are biological realistic ingredients absent in the fully connected Hopfield model.

In order to introduce asymmetry in the connections, the synapses J_{ij} and J_{ji} are cut with probability $1 - C/N$ independently of each other [3], where C is the mean connectivity of each neuron and the extreme dilution limit is obtained when $C \ll \ln N$ (N is the size of the network).

Measuring the network load by $\alpha = P/C$, where P is the number of stored patterns, Derrida, Gardner and Zippelius (hereafter DGZ) found that there is a critical value $\alpha_c = 2/\pi$ above which the system cannot retrieve the stored information. Since the storage capacity is here measured by the amount of bits that can be stored (PN) per synapse (CN), in the diluted version the Hopfield model is more efficient than the fully connected case ($C = N$) in which $\alpha_c \simeq 0.138$ [4].

Synapses connecting more than two neurons can be considered to both improve the storage capacity of the network [5]-[11] and to mimic real synapses existing in nervous systems (see [5] and references therein). For instance, axon-axon-dendrite connections can be described as third order synapses (even more intricate connections, involving more than two axons, may also exist in the brain) [5]. Moreover, when some pairwise connections are close enough, they may interact somehow, and that can also be considered as high (even) order synapses. Diluted networks with high order connections were studied in refs. [7,8,9]. Kanter [7] and Tamarit *et al* [8] considered a monomial of order k in the overlap and found a discontinuous transition at $\alpha_c(k)$ for $k > 2$. Also, in the (α, T) phase diagram the retrieval phase shrinks as k increases: $\alpha_c(k) \to 0$ as $k \to \infty$ although the retrieval is perfect ($m \to 1$). Wang and Ross [9] treated instead a polynomial, controlling the relative coefficients (weights) and found, besides a retrieval phase, regions where the system can be either periodic or chaotic, depending on the noise or the degree of parallelism in the updating.

In this paper we study the dynamical effects of introducing a correction term to the Hopfield model [11] in the extreme dilution limit of both, two and fourth order synapses. The difference between our model and those studied by Kanter *et al* [7], Tamarit *et al* [8] and Wang *et al* [9] lays in the nature of high order connections we consider (see details below). The paper is organized as follows: section 2 reviews the model and in sections 3 and 4 analytical and

numerical results are presented for the dynamics. In section 5 we summarize and present our conclusions.

2 THE TRUNCATED MODEL

In a binary neural network, as for example the Hopfield model[12,13], each neuron is modeled by an Ising variable S_i that can take the values $\{+1,-1\}$ representing the active and passive state, respectively. Possible states of the network are given by N-dimensional vectors $\vec{S} \in \{+1,-1\}^N$ and the embedded memories are associated to P of these states, denoted by $\vec{\xi}^\mu$ $(\mu = 1,\ldots,P)$.

The fully connected Truncated model can be regarded as the Hopfield model plus correction terms. Since the synapses are symmetric, the dynamics is ruled by a Lyapunov function (called Hamiltonian by analogy with magnetic systems) and the long time behavior of the network can be inferred from a thermodynamical analysis of the system. In this case the Hamiltonian is given by [10,11]

$$\begin{aligned}\mathcal{H} &= \frac{N}{2}\sum_{\ell=1}^{M}(-1)^{\ell}\varepsilon_{2\ell}\sum_{\mu_1<\ldots<\mu_\ell} m_{\mu_1}^2 m_{\mu_2}^2\ldots m_{\mu_\ell}^2 \\ &= -\varepsilon_2\frac{N}{2}\sum_{\mu_1} m_{\mu_1}^2 + \varepsilon_4\frac{N}{2}\sum_{\mu_1<\mu_2} m_{\mu_1}^2 m_{\mu_2}^2 - \ldots + (-1)^M\varepsilon_{2M}\frac{N}{2}\sum_{\mu_1<\ldots<\mu_M} m_{\mu_1}^2\ldots m_{\mu_M}^2 \quad (1)\end{aligned}$$

where $2M$ is the highest order of interaction and the overlap m_μ between the state of the network $\vec{S}$ and the pattern $\vec{\xi}^\mu$ is given by

$$m_\mu = \frac{1}{N}\sum_{i=1}^{N}\xi_i^\mu S_i \quad . \qquad (2)$$

In what follows we consider only the first correction to the Hopfield term ($M = 2$ and $\varepsilon_{2\ell} = \delta_{1\ell} + \epsilon\delta_{2\ell}$). Eq.(1) can then be rewritten as

$$\mathcal{H} = -\frac{1}{2}\sum_{i,j} J_{ij}S_iS_j + \frac{\epsilon}{2}\sum_{i,j,k,l} J_{ijkl}S_iS_jS_kS_l \quad . \qquad (3)$$

The learning rule for the second order J_{ij} and fourth order J_{ijkl} follows directly from eq.(1) and will be detailed in the next section [13].

The equilibrium statistical mechanics [4] of this model was studied in refs. [11], showing an extremely rich behavior that depends on the value of ϵ. The main features of the system at $T = 0$ (for non zero temperatures the behavior is analogous) are summarized by the phase diagram

in fig.1: for large ϵ (~ 0.5) the overlap m decreases continuously with α, going monotonically from 1 down to zero at $\alpha_c^+(\epsilon)$; as ϵ decreases (~ 0.36), the overlap presents a local minimum, before finally going to zero at $\alpha_c^+(\epsilon)$. If $\epsilon < \epsilon_c \simeq 0.3587$, the minimum yields a gap separating two retrieval regions. Not too close to ϵ_c the gap Δ has a discontinuous border at α_c' and a continuous one at α_c^-. The points where m continuously approaches zero, $\alpha_c^\pm(\epsilon)$, are

$$\alpha_c^\pm(\epsilon) = \left(\frac{1}{\sqrt{\epsilon}} \pm \sqrt{\frac{2}{\pi}}\right)^2 \quad . \tag{4}$$

As $\epsilon \to 0$, $\Delta \equiv \alpha_c^-(\epsilon) - \alpha_c'(\epsilon)$ goes to infinity as ϵ^{-1}. Thus, when the Truncated model recovers the Hopfield model ($\epsilon \to 0$), the location of the second retrieval region in the α-axis goes to infinity and $\alpha_c'(0) \simeq 0.138$. Numerical simulations [11] at $T = 0$ show the above transitions and the existence of the gap. The basins of attraction seem to be large and α-independent; the mean convergence time increases with α and, for non small values of α, does not depend on the initial overlap.

There is also an optimal value of ϵ that strongly improves the storage capacity of the model by canceling the noise term for each value of α [11]:

$$\epsilon_{opt} = \frac{1}{1+\alpha} \quad . \tag{5}$$

As we will see in the next two sections, there is an analogue of this optimal value for the diluted network. A complete discussion of these and other results for the fully connected Truncated model can be found in refs.[11].

3 THE DILUTED NETWORK

In this section we study the dynamics of an extremely diluted and asymmetric version of the network described in section 2 in two different cases: the initial state has a macroscopic overlap with a) only one pattern and b) two correlated patterns (out of $P-2$ uncorrelated ones). Due to the asymmetry in the connections, a Lyapunov function can no longer be defined for the network and hence we are constrained to study the time evolution of the system ruled by the Heat Bath dynamics, given by

$$S_i(t+\Delta t) = \begin{cases} +1 \text{ with probability } (1+\exp[-2\beta_o h_i(t)])^{-1} \\ \\ -1 \text{ with probability } (1+\exp[+2\beta_o h_i(t)])^{-1} \end{cases} \tag{6}$$

where the parameter $\beta_o \equiv T_o^{-1}$ (called the inverse of the temperature) measures the noise level of the net and $h_i(t)$ is the local field acting on the neuron i at time t:

$$h_i = \sum_j J_{ij} S_j - \epsilon \sum_{j,k,l} J'_{ijkl} S_j S_k S_l \quad . \tag{7}$$

Based on eq.(1), the couplings are:

$$J_{ij} = C_{ij} \sum_\mu \xi_i^\mu \xi_j^\mu \tag{8}$$

$$J'_{ijkl} = \frac{1}{3}\left(J_{ijkl} + J_{ljki} + J_{kjil}\right) \tag{9}$$

$$J_{ijkl} = C_{ijkl} \sum_{\mu \neq \nu} \xi_i^\mu \xi_j^\mu \xi_k^\nu \xi_l^\nu \tag{10}$$

and C_{ij} and C_{ijkl} are random variables distributed according to the probabilities ρ and $\tilde{\rho}$:

$$\begin{aligned} \rho(C_{ij}) &= \frac{C}{N}\delta(C_{ij}-1) + \left(1-\frac{C}{N}\right)\delta(C_{ij}) \\ \tilde{\rho}(C_{ijkl}) &= \frac{C}{N^3}\delta(C_{ijkl}-1) + \left(1-\frac{C}{N^3}\right)\delta(C_{ijkl}) \end{aligned} \tag{11}$$

where $C \ll \log N$. The asymmetry is introduced through the independence of C_{ij} and C_{ji} (the same holds for C_{ijkl}).

In the fully connected case some of the self-connections are not zero, particularly, J_{iikl} and J_{ijkk}. These self-interactions create correlations between the states of neuron i at different times, that is, $\langle S_i(t) S_i(t') \rangle \neq 0$, what apparently prevents from using the DGZ prescription to obtain the time evolution of the diluted network. Actually, it can be proved that the field generated by the self-interactions vanishes in the thermodynamical limit, implying null correlations.

Assuming that the updating is parallel and the initial state is correlated with only one of the embedded memories, we are interested in obtaining a recurrent equation,

$$m(t+1) = f(m(t)) \quad ,$$

for the overlap $m(t)$ between the state of the network and this memory,

$$m(t) = \frac{1}{N}\sum_i \langle \xi_i^1 S_i(t) \rangle \quad , \tag{12}$$

where $\langle \ldots \rangle$ denotes both thermal and configuration averages. Using standard techniques and considering non biased patterns, after taking the limit of $C \to \infty$, the equation ruling the parallel evolution of the system reads:

$$m(t+1) = \int_{-\infty}^{+\infty} \mathcal{D}y \, \tanh \beta \left[m(t) - \sqrt{2\alpha} y (1 - \epsilon m^2(t)) \right] \quad , \tag{13}$$

where $C\alpha = P - 1$, $\beta = C/T_o$ and $\mathcal{D}y$ is the gaussian measure:

$$\mathcal{D}y = \frac{dy}{\sqrt{\pi}} e^{-y^2} \quad . \tag{14}$$

We also study the case where the initial state has a macroscopic overlap only with the two first memories, which have a fixed overlap between them,

$$\kappa = \frac{1}{N} \sum_i \xi_i^1 \xi_i^2 \quad , \tag{15}$$

the remaining $P - 2$ being uncorrelated. The quantities of interest are then the overlaps with these two memories:

$$\begin{aligned} m_1(t) &= \frac{1}{N} \sum_i \langle \xi_i^1 S_i(t) \rangle \\ m_2(t) &= \frac{1}{N} \sum_i \langle \xi_i^2 S_i(t) \rangle \end{aligned} \tag{16}$$

and the time evolution equations for them are ruled by:

$$M(t+1) = (1+\kappa) \int \mathcal{D}y \, \tanh \beta \left[M \left(1 - \epsilon \frac{(M^2 - m^2)}{4} \right) - y\sqrt{2\alpha} \left(1 - \frac{\epsilon (M^2 + m^2)}{2} \right) \right] \tag{17}$$

$$m(t+1) = (1-\kappa) \int \mathcal{D}y \, \tanh \beta \left[m \left(1 + \epsilon \frac{(M^2 - m^2)}{4} \right) - y\sqrt{2\alpha} \left(1 - \frac{\epsilon (M^2 + m^2)}{2} \right) \right]$$

where:

$$\begin{aligned} M &= m_1 + m_2 \\ m &= m_1 - m_2 \quad . \end{aligned} \tag{18}$$

In the next section the above equations are numerically solved and the results with their interpretation are presented.

4 RESULTS

In the $T = 0$ limit, $f(m)$ becomes

$$f(m) = \mathrm{erf}\left[\frac{m(t)}{\sqrt{2\alpha}(1 - \epsilon m^2(t))}\right] \quad . \tag{19}$$

Fig.2 displays this map for two different values of ϵ showing that for $\epsilon < 1$ it is continuous while it is discontinuous otherwise.

In fig.3 we show the fixed points of the equation $m(t+1) = f(m(t))$ as a function of α for several values of $\epsilon < 1$. For $\epsilon < 0.266$ the system has only a fixed point that decreases continuously down to 0 at $\alpha_c = 2/\pi$. Above this critical value, there is only the $m = 0$ solution. For $0.266 < \epsilon < 1$ the transition is discontinuous and α_c is greater than $2/\pi$, increasing with ϵ. In this case there are three different regimes: for $\alpha < 2/\pi$ there is only the retrieval solution; for $2/\pi < \alpha < \alpha_c$ this solution coexist with the $m = 0$ one and for $\alpha > \alpha_c$ there is only the paramagnetic solution. In the intermediate regime, an unstable solution appears that separates the basins of attractions of the two stable solutions and the retrieval basin decreases with α as can be seen in fig.3. Also, for a given value of α, the closer ϵ is to 1 the better is the retrieval. The retrieval region below the line α_c, where exists a nonzero fixed point, is named R_1, while above α_c the paramagnetic phase is named P.

At $\epsilon = 1$ there always is the solution $m = 1$ and the unstable solution found for $\alpha > 2/\pi$ drops to zero as we approach $\epsilon = 1$. Hence, the basin of attraction of the retrieval solution increases while the basin of the paramagnetic solution shrinks to zero when $\epsilon \to 1$. This means that the network *capacity diverges* and the *retrieval is perfect* for all nonzero initial states! This behavior is the analogue of the ϵ_{opt} found in the fully connected system where $\epsilon = (1+\alpha)^{-1}$ while here we have

$$\epsilon_{opt} = \frac{1}{1 + P/N} \simeq \frac{1}{1 + \alpha C/N} = 1 \quad , \tag{20}$$

since $C \ll \ln N$.

For values of $\epsilon > 1$ a rich behavior emerges and the system presents a novel kind of retrieval. The overall behavior of the system is presented in fig.4, showing several regimes. For a fixed ϵ and low values of α the system is in a retrieval phase (R_2) where it oscillates between a state with overlap m with the pattern and a state with $-m$ overlap.

As α increases the system enters in a new phase. It starts oscillating between two distinct values of m, say m_1 and m_2 ($|m_1| \neq |m_2|$) while higher periods appear with increasing values of α leading to a chaotic regime. The route to chaos followed by the system is not exactly period doubling since it suffers split bifurcations [14]: before doubling the period of the attractor, the system doubles the number of stable attractors. For instance, a period 2 cycle splits in two period 2 cycles before becoming a period 4 one. The transition from the twofold attractor to the double period one occurs when the system enters a superstable orbit (those that contain the critical points). This behavior is very similar to that found in the cubic logistic map $f(m) = \alpha m(1-m^2)$ where only one split bifurcation is allowed in the periodic region (a system with two critical points can only have two stable attractors) [14]. A representative behavior of the system is shown in fig.5. The basins of each attractor for $\alpha = 0.6$ and $\varepsilon = 2$ were also examined: for an initial value of m around 0 the domains are extremely mixed. This behavior is better understood if one plots the function iterated several times (e.g., 16) as a function of m (fig. 6): the function $f^{(16)}$ is a set of discontinuous plateau at some values of m.

To decide whether a given temporal sequence is chaotic or not we calculated the Lyapunov exponent through its definition

$$\lambda \equiv \lim_{n\to\infty} \frac{1}{n} \sum_{i=1}^{n} \ln |f'(m_i)| \tag{21}$$

where n is the length of the sequence. In the aperiodic regime one has $\lambda > 0$ indicating that the system is chaotic while if its behavior is periodic, $\lambda < 0$. It is worth noting that even in the periodic and in the chaotic attractors, the system always passes very close to the memorized pattern, as can be observed in fig.5 for $\varepsilon = 2$. We have verified numerically that for any point in this phase (C), the attractors have at least one point with overlap m near 1, hence it is possible to interpret this cyclic or chaotic phase as an alternative retrieval phase, in which the system does not recognize a memory by reaching a fixed point but by wandering around it.

For large enough α the system enters a paramagnetic phase (the only fixed point of eq.(19)) as can be observed in the phase diagram fig.4. Notice also the similarities between the $T = 0$ phase diagram for the diluted and the fully connected system: both have a retrieval region around the optimal value of ε for all values of α due to the canceling of the noise term. The difference is that in the fully connected model $\varepsilon_{opt} = \varepsilon_{opt}(\alpha)$ while in the diluted one it is a constant. Also, in the fully connected case there is not a chaotic phase (not even a periodic one) because there the connections are symmetric allowing the introduction of a Lyapunov function (the Hamiltonian eq.(1)). We have also determined that, as $\varepsilon \to 1$

$$\alpha_c \sim |1-\varepsilon|^{-2} \quad . \tag{22}$$

Figure 7 displays the T versus α phase diagram for $\varepsilon \leq 1$ where there are only fixed point attractors: one with $m = 0$ (P) and another with $m \neq 0$ (R_1). In particular, for values of ε where the transition is continuous the line T_c is independent of ε and satisfies

$$\beta_c \int_{-\infty}^{+\infty} \mathcal{D}y \operatorname{sech}^2 \left[\beta_c y \sqrt{2\alpha}\right] = 1 \quad . \tag{23}$$

If $\varepsilon > 1$, the map eq.(13) presents a solution with $m = \pm\varepsilon^{1/2}$ at

$$\beta^* = \frac{\sqrt{\varepsilon}}{2} \ln \frac{\sqrt{\varepsilon}+1}{\sqrt{\varepsilon}-1} \quad . \tag{24}$$

It means that for $T = T^* = (\beta^*)^{-1}$ the system presents the above solution for all values of α. In the limit $\varepsilon \to 1$, $T^* = 0$ and $m = \pm 1$, as is shown in fig.4 and, as $\varepsilon \to \infty$, $T^* \to 1$. In fig.8 the T versus α phase diagram for $\varepsilon = 2$ is shown. Note that, besides the three phases appearing at $T = 0$, we now found also an R_1 phase even for $\varepsilon > 1$. For increasing values of α the $m = 0$ region dominates except for points around T^*. In fig.9 the behavior of m for $\varepsilon = 2$ and $\alpha = 1$ is shown as a function of T with the corresponding Lyapunov exponent λ. Note the backward period bifurcation leading to a retrieval phase for high temperatures: the system leaves the chaotic regime and become periodic as the temperature increases until a certain temperature where it has a fixed point and is able to retrieve the stored information.

Finally we have analyzed the case in which only two memories have macroscopic overlap κ, being the dynamics ruled by eq.(18), starting always from the initial condition $m_1(0) = 1$ and $m_2(0) = \kappa$. The attractors of these equations were numerically studied and four different phases were distinguished: a retrieval one (R_1) which correspond to a fixed point with $|m_1| > |m_2| > 0$, another retrieval phase (R_2) in which the system oscillates in a cycle two between the states with $|m_i| = cte$, $|m_1| > |m_2|$, a mixed phase (M) with $m_1 = m_2 \neq 0$, a paramagnetic phase (P) with $m_1 = m_2 = 0$ and a cyclic or chaotic one (C).

For $\alpha = 0$, when one considers macroscopic overlap with only one pattern, the DGZ equation is recovered. But, in the situation where the system has macroscopic overlap with two memories we do not recover the DGZ equations, that is, there is still an ε dependence on the equations. Surprisingly, this also holds for $\kappa = 0$: the system may present a cyclic or chaotic regime, absent if one looks for a retrieval solution. In fig.10 we present the phase diagram T versus ε for $\kappa = 0.2$ and $\alpha = 0$. For $T = 0$ the system present only two phases: the retrieval one for $|\varepsilon| < \kappa^{-1}$ and the cyclic and chaotic one for $|\varepsilon| > \kappa^{-1}$, while the mixed phase appears for a given temperature that depends on the value of κ. It is important to stress that the boundary between the retrieval phase and the cyclic or chaotic one for positive ε shows the first appearance of cyclic orbits: inside the C phase there are islands of retrieval. Also, in the

boundary between the mixed phase and the paramagnetic one, there is a point ϵ^*, above which the transition is continuous and discontinuous below. It can be shown that the transition line in the continuous case is given by $T_c = 1 + \kappa$.

In the case $\alpha \neq 0$ and $T = 0$, the α versus ϵ phase diagram is shown in fig.11. This phase diagram is qualitatively similar to the one where there is overlap with only one memory (fig.4). There is also an value of ϵ where the capacity diverges, but here it is given by

$$\epsilon_{opt} = 1 - \kappa^2 \quad . \tag{25}$$

Besides that, the boundary between the paramagnetic phase and the mixed one is

$$\alpha_c = \frac{2}{\pi}(1 + \kappa)^2 \quad . \tag{26}$$

In the line $\alpha = 0$ of R_2 region on the above diagram, there is always the retrieval solution R_1.

5 CONCLUSIONS

We presented an exact solution for the dynamics of a model for neural networks with high order interactions that shows a very rich behavior depending on the parameters α, ϵ and T. In analogy with the related fully connected model, there is an optimal value of ϵ for which the model always retrieves the embedded information (although the process may not be perfect). It is important to stress that for some values of ϵ the retrieval region is found at high values of T: amazingly, as the temperature is decreased, the system passes from an disordered phase (P) to an ordered one (R) and, after passing through a region where it presents cyclic or chaotic orbits, it reenters in the paramagnetic region. In this case, the presence of thermal noise may improve the retrieval abilities of the system.

The periodic or chaotic behavior is only present for $\epsilon > 1$. Apparently, the reason for this is that below $\epsilon = 1$ the Hopfield second order term surpass the fourth order one while for $\epsilon > 1$ it is the reverse. In the later case, due to the asymmetry on the synapses (the presence of both μ and ν in the learning rule), cycles are introduced. This is analogous to some models where the task is to retrieve temporal sequences [16] and the learning rule explicitly stores the transitions between states. The absence of this kind of transition in the fully connected model is due to the possibility of symmetrization of all the connections, and hence allowing the introduction of an energy function for the system. Also, if $\epsilon < 1$ the map eq.(13) is invertible and continuous, not allowing chaos for one dimensional systems [19].

Due to the very complex nature of the system behavior, it would also be interesting to study the thermodynamics of the symmetric diluted case [17], trying to see the interplay between the

fully connected case and the highly diluted one. Also, if chaos can be controlled as proposed by Ott, Grebogi and Yorke [18], the phase boundaries of the above phase diagrams may change, increasing the retrieval region.

The presence of the mixed (M) phase is an indication that the study of the generalization abilities of the model may reveal some interesting features.

At last, a remark on the possible role of chaos on the problem of perception and recognition is worth. It was proposed [15] that the property of large groups of neurons changing abruptly their activity pattern due to small inputs is responsible for the flexibility of real nervous systems to create new patterns when interacting with the outside world, flexibility that may underlie the learning and creative processes.

Acknowledgments: We acknowledge R.M.C. de Almeida for several interesting discussions and for encouraging this work. Also, we are in debt with J.C.M. Mombach, F.B. Rizatto, D. Stariolo and C. Tsallis for useful discussions. F.T.A. acknowledges the kind hospitality of the IF-UFRGS during his stay at Porto Alegre. Work partially supported by brazilian agencies Conselho Nacional de Desenvolvimento Científico e Tecnológico (CNPq), Financiadora de Estudos e Projetos (FINEP) and Fundação de Amparo à Pesquisa do Estado do Rio Grande do Sul (FAPERGS).

Figure Captions

Figure 1: Phase diagram α versus ϵ at $T = 0$ of the fully connected Truncated model. The lines $\alpha_c^{\pm}$ are second order while α_c' is discontinuous.

Figure 2: Right hand side of eq.(19) for $\alpha = 0.5$ and two values of ϵ: 0.5 (dashed) and 2 (solid).

Figure 3: Fixed points m versus α for several values of ϵ. The solid line is for stable solutions while the dashed is for unstable ones. For $\alpha > 2/\pi$ the paramagnetic solution is always stable.

Figure 4: Phase diagram α versus ϵ at $T = 0$ for the diluted Truncated model. The transition is continuous for $\epsilon < 0.266$. The optimal value of ϵ is 1 where $\alpha_c \to \infty$ as $|1 - \epsilon|^{-2}$. For $\epsilon > 1$ the system can present a periodic or chaotic phase (C) and a retrieval one (R).

Figure 5: Plot of m versus α at $T = 0$ for $\epsilon = 2$. For high values of ϵ there is only the $m = 0$ solution while for lower values of ϵ the system behavior is complex.

Figure 6: Map eq.(13) iterated 16 times showing the existence of several plateau for $\epsilon = 2$ and $\alpha = 0.6$.

Figure 7: Phase diagram for some values of $\epsilon < 1$ showing the existence of only two phases: a retrieval one ($T < T_c$) and $m = 0$ one ($T > T_c$). For $\epsilon < 0.266$ the line T_c is the same as of the case $\epsilon = 0$.

Figure 8: Phase diagram for $\epsilon = 2$. The retrieval (R) and the periodic or chaotic phases (C) are surrounded by the $m = 0$ one (P). Note that for $T^* \simeq 0.8$ the system has the solution $m = \pm 1/\sqrt{2}$ for all values of α.

Figure 9: The overlap m versus T for $\epsilon = 2$ and $\alpha = 2$ and the corresponding Lyapunov exponent. The system has only a retrieval regime at high temperatures.

Figure 10: Phase diagram for $\alpha = 0$ and $\kappa = 0.2$ in the case where there is macroscopic overlap with two memories (see text).

Figure 11: Phase diagram for $T = 0$ and $\kappa = 0.2$ in the case where there is macroscopic overlap with two memories (see text). Below the R_2 phase, at $\alpha = 0$, the system is in an R_1 phase, and that below M, in a C phase. This compatibilizes this diagram with the former one (fig.10).

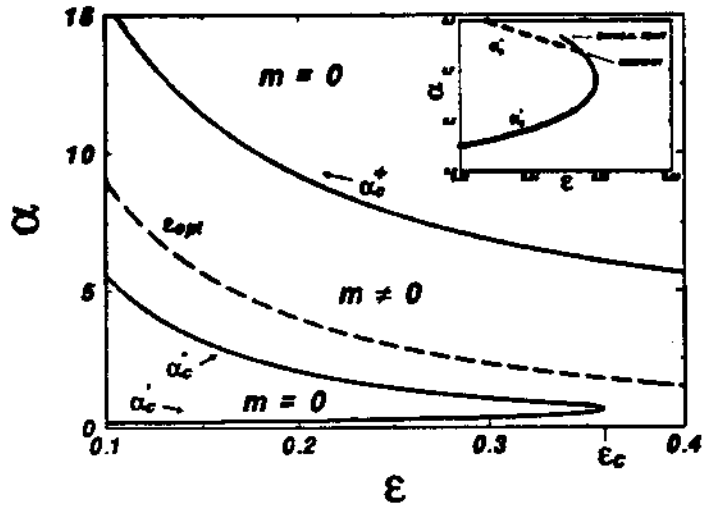

Fig. 1

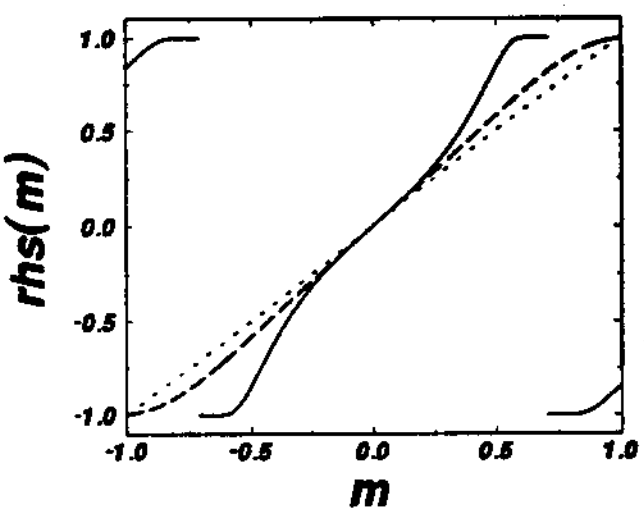

Fig. 2

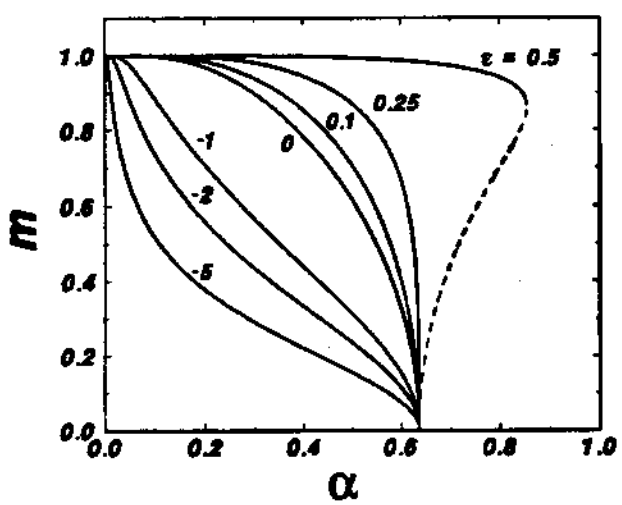

Fig. 3

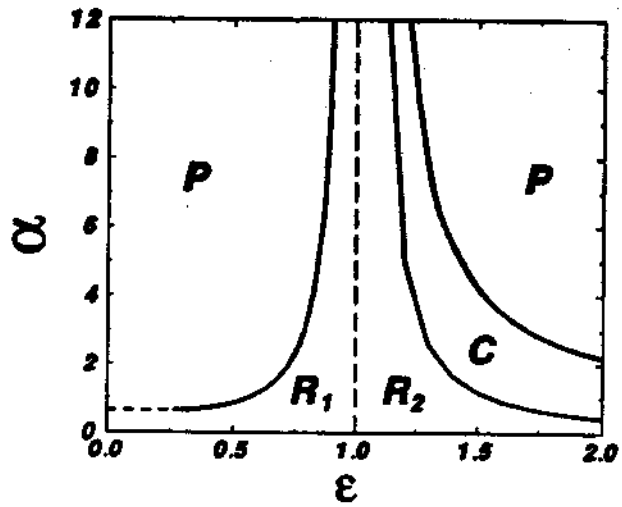

Fig. 4

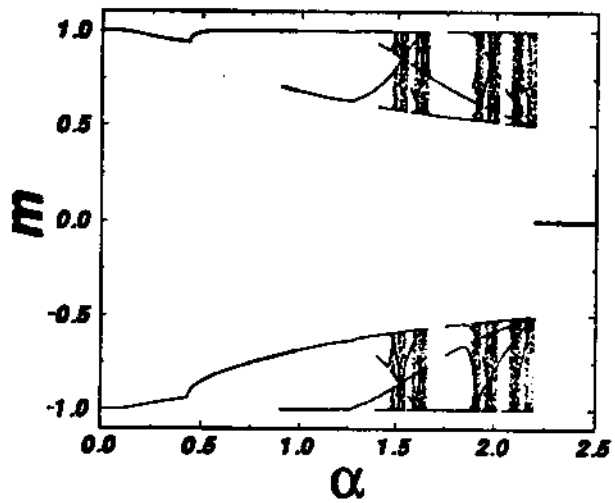

Fig. 5

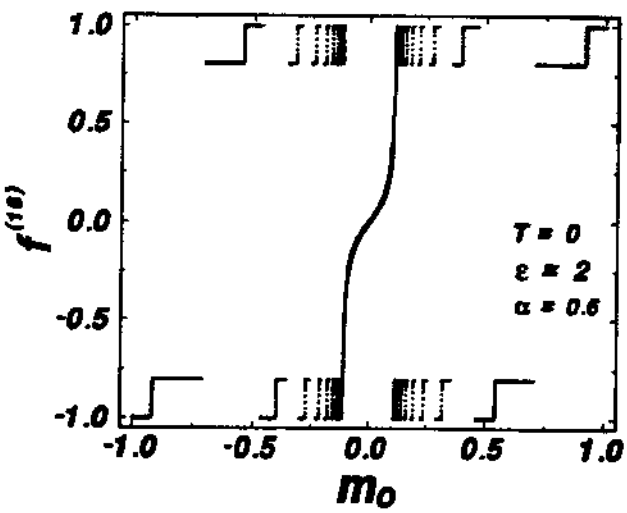

Fig. 6

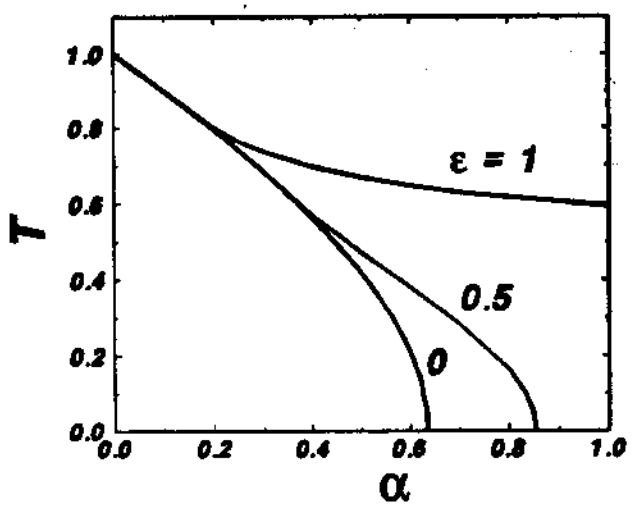

Fig. 7

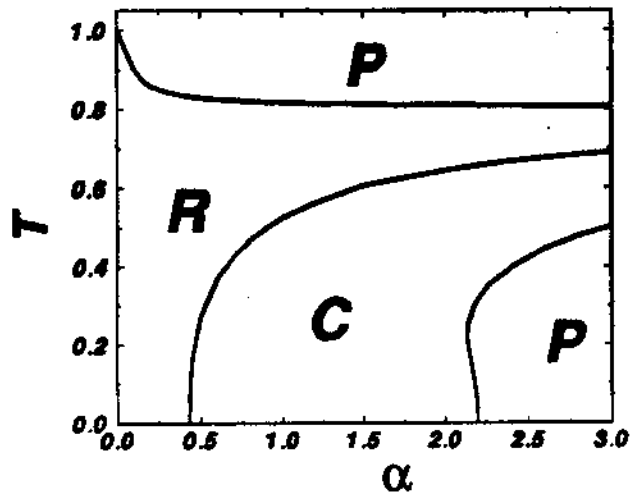

Fig. 8

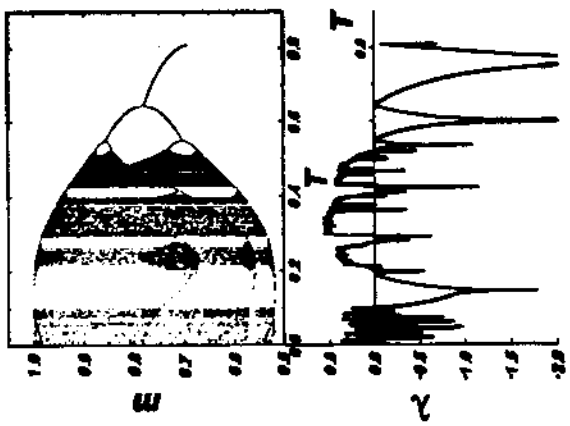

Fig. 9

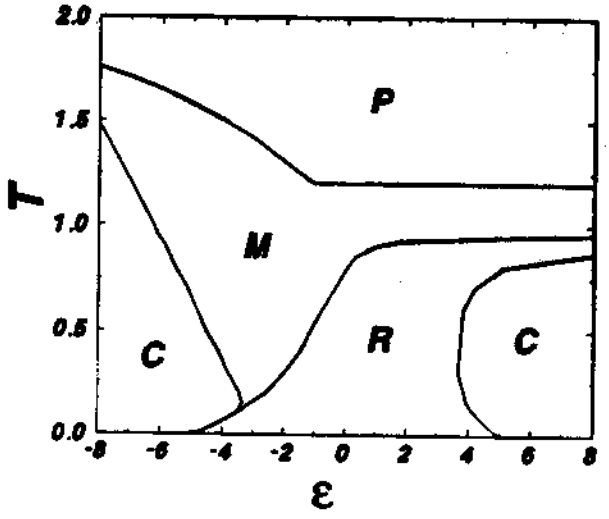
2.0
1.5
1.0
0.5
0.0
T
P
M
C
R
C
-8
-6
-4
-2
0
2
4
6
8
ε

Fig. 10

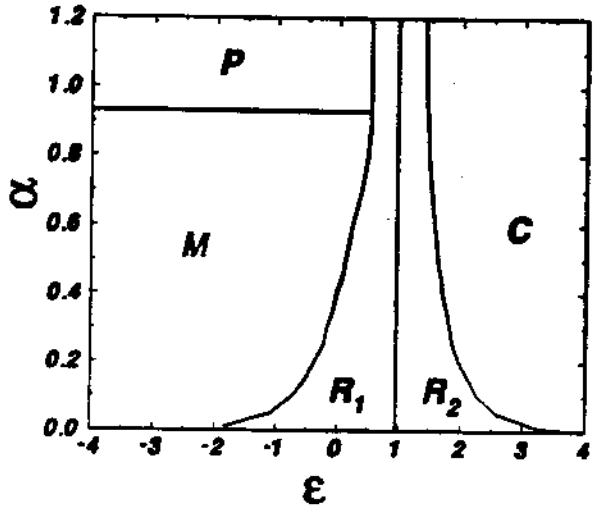
1.2
1.0
0.8
0.6
0.4
0.2
0.0
α
P
M
C
R1
R2
-4
-3
-2
-1
0
1
2
3
4
ε

Fig. 11

References

[1] COOLEN A.C.C. AND RUIJGROK TH.W. 1988 Phys. Rev. **A38** 4253
KEPLER T.B. AND ABBOTT L.F. 1988 J. Phys. France **49** 1657
GARDNER E., DERRIDA B. AND MOTTISHAW P. 1987 J. Phys. France **48** 741

[2] PATRICK A.E. AND ZAGREBNOV V.A. 1991 J. Phys. **A24** 3413

[3] DERRIDA B., GARDNER E. AND ZIPPELIUS A. 1987 Europhys. Lett. **4** 167

[4] AMIT D.J., GUTFREUND H. AND SOMPOLINSKY H. 1987 Ann. Phys. NY **173** 30

[5] PERETTO P. AND NIEZ J.J. 1986 Biol. Cybern. **54** 53

[6] GARDNER E. 1987 J. Phys. A **20** 3453
ABBOTT L.F. AND ARIAN Y. 1987 Phys. Rev. **A36** 5091
HORN D. AND USHER M. 1988 J. Phys. France **49** 389

[7] KANTER I. 1988 Phys. Rev. **A38** 5972

[8] TAMARIT F.A., STARIOLO D.A. AND CURADO E.M.F. 1991 Phys. Rev. **A43** 7083

[9] WANG L. AND ROSS J. 1991 Phys. Rev. **A44** R2259

[10] DE ALMEIDA R.M.C. AND IGLESIAS 1990 Phys. Lett. A **146** 239
ARENZON J.J., DE ALMEIDA R.M.C. AND IGLESIAS J.R. 1992 J. Stat. Phys. **69** 385

[11] ARENZON J.J., DE ALMEIDA R.M.C., IGLESIAS J.R., PENNA T.J.P. AND DE OLIVEIRA P.M.C. 1993 Physica A **197** 1
ARENZON J.J. AND R.M.C. DE ALMEIDA 1993 Phys. Rev. **E48** 4060

[12] HOPFIELD J.J. 1982 Proc. Natl. Acad. Sci. USA **79** 2554

[13] HERTZ J., KROGH A. AND PALMER R.G. 1991 Introduction to the Theory of Neural Computation (Addison-Wesley Publishing Company)

[14] TESTA J. AND HELD G.A. 1983 Phys. Rev. **A28** 3085

[15] SKARDA C.A. AND FREEMAN W.J. 1987 Behavioral and Brain Sciences **10** 161

[16] For a review see KUHN R. AND VAN HEMMEN J.L. in "Physics of Neural Networks" (E. Domany, J.L. van Hemmen and K. Schulten eds.), Springer 1990.

[17] CANNING A. AND GARDNER E. 1988 J. Phys. **A21** 3275

[18] OTT E., GREBOGI C. AND YORKE J. 1990 Phys. Rev. Lett. **64** 1196

[19] OTT E. 1993 Chaos in Dynamical Systems (Cambridge University Press)